LARS DB67 0185

A Shock-Induced Phase Transformation in Bismuth†

DONALD B. LARSON

Lawrence Radiation Laboratory, University of California, Livermore, California

(Received 20 June 1966; in final form 26 October 1966)

A study was made of the shock-induced phase transformation in bismuth at 25 kbar. A quartz pressure-gauge technique was used to obtain the experimental data. A previously reported disagreement between the dynamic and the static transition pressure is due in part to a strength-of-material correction. The remaining discrepancy is probably due to a systematic error in the earlier dynamic study. The observed dynamic transition pressures corrected for strength-of-material effects and corrected to 25°C were 25.4 kbar for isotropic bismuth, and 25.9 kbar for cast bismuth. These values agree nicely with the value 25.4 kbar obtained by static compression. Hugoniot elastic limits of 2.4 to 3.1 kbar were observed for the different types of samples.

INTRODUCTION

THE possibility of observing a shock-induced solid–solid phase transformation during the microsecond observation time of a dynamic experiment was first demonstrated by Bancroft *et al.*[1] in 1956. This first shock-induced transformation was observed in iron at a pressure near 130 kbar. Before the iron transition was verified statically, Duff and Minshall[2] investigated a dynamically induced phase transformation in bismuth at pressures near 25 kbar. This was undoubtedly the Bi I to Bi II transformation observed statically by Bridgman,[3] since Duff and Minshall reported an experimentally determined phase line with a slope of −50.8 bar/°C, which compares favorably with the value of −50.0 bar/°C reported by Bridgman. However, the dynamically determined phase line was shifted, giving pressures 2.7 kbar higher than the corresponding static phase line. Duff and Minshall suggested two possible explanations for this disagreement. First, bismuth has a residual strength at the transition, and therefore the apparent pressure in the shock experiment is greater than the effective hydrostatic pressure. The second possible explanation was that there is something different about the detailed mechanism of shock-induced transformations, and it was conjectured that the nucleation process might therefore require a greater activation energy and thus a greater pressure in the dynamic experiment.

This observed but unexplained difference in dynamically and statically determined transition pressures in bismuth was the motivation for the present detailed study of bismuth under shock loading. A new experimental technique with quartz pressure gauges was selected to allow an independent approach to the experimental data.

THEORETICAL CONSIDERATIONS

The interpretation of data extracted from dynamic studies is based on certain assumptions. First of all one assumes that thermodynamic equilibrium exists in the sample behind the shock front. This assumption requires that equilibrium be established in the sample in time of the order of 10^{-6} sec. Experimentally, this assumption appears to be valid in most cases.[4] A second basic assumption often made is that strength-of-materials effects are negligible, and thus the dynamically determined pressure is just the effective hydrostatic value. Experimental data indicates that this second assumption is generally valid at pressures above 100 kbar. Deviations from this assumption are often approximated by using sample yield strength data and some type of elastic-plastic model to correct the observed pressures to effective hydrostatic values.[5]

In a study of a dynamic phase transformation, these basic assumptions are important.[6] To measure a pressure that characterizes a material at a phase line, thermodynamic and hydrodynamic equilibrium must be attained in times of the order of a microsecond. Any transient behavior that delays equilibrium must be carefully evaluated experimentally for each material studied.

Shock-Induced Phase Transformations

A qualitative description of the Hugoniot of a material undergoing a shock-induced first-order phase transformation was presented by Bancroft *et al.*[1] Figure 1 is a hypothetical Hugoniot for a material which undergoes such a transition and also exhibits a finite strength. Point A is the elastic yield point for dynamic loading and is often referred to as the Hugoniot elastic limit. At point B the Hugoniot meets the phase line. The formation of phase-II material at this boundary produces the cusp shown in Fig. 1. For some range of pressures above point B, a mixed-phase region is produced along the Hugoniot because of the non-isothermal nature of the shock experiment. From a hydrodynamic point of view, this hypothetical

† Work performed under the auspices of the U.S. Atomic Energy Commission.

[1] D. Bancroft, E. L. Peterson, and F. S. Minshall, J. Appl. Phys. **27**, 291 (1956).

[2] R. E. Duff and F. S. Minshall, Phys. Rev. **108**, 1207 (1957).

[3] P. W. Bridgman, Phys. Rev. **48**, 896 (1935).

[4] M. H. Rice, R. G. McQueen, and J. M. Walsh, in *Solid-State Physics*, F. Seitz and D. Turnbull, Eds. (Academic Press Inc., New York, 1958), Vol. 6, pp. 1–63.

[5] G. R. Fowles, J. Appl. Phys. **32**, 1475 (1961).

[6] B. Alder, *Solid Under Pressure*, W. Paul and D. Warschauer, Eds. (McGraw-Hill Book Company, Inc., New York, 1963), pp. 385–427.

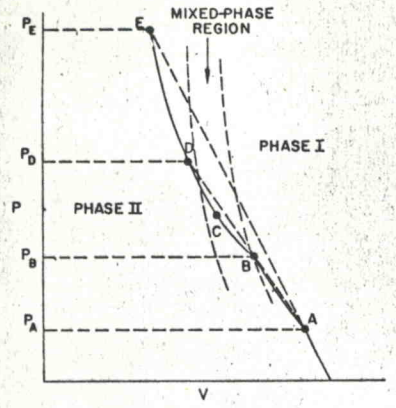

FIG. 1. Hugoniot for a hypothetical material which has an elastic yield point (point A) and a phase transformation (point B).

material will exhibit shock instability at both point A and point B. These shock instabilities give rise to a steady-state multiple-wave structure which can be analyzed experimentally to determine points A and B.

The various points along a Hugoniot are related through the Hugoniot conservation relations

$$\frac{V}{V_0}=\frac{\rho_0}{\rho}=\frac{(U_s-U_p)}{(U_s-U_{p0})}$$

conservation of mass (1)

$$P-P_0=\rho_0(U_s-U_{p0})(U_p-U_{p0})$$

conservation of momentum (2)

and

$$E-E_0=\tfrac{1}{2}(P+P_0)(V_0-V)$$

conservation of energy, (3)

where ρ is density, V is specific volume, P is pressure, U_s is shock velocity, U_p is particle velocity, and E is specific internal energy, and where zero-subscripted variables refer to an initial state on the Hugoniot, and the nonsubscripted variables to a second state accessible from the first state. Experimental measurement of any two of the parameters P, U_p, U_s, V, and E which characterize a shock wave will determine, through the conservation relations, the other properties of the compressed material immediately behind the wave.

Duff and Minshall[2] presented an extension of this earlier work by Bancroft *et al.* when they showed that knowledge of the slope of the Hugoniot above point B and the isothermal compressibility below B provides a measure of the phase-line slope for the transition. They also conjectured on the characteristics of the transient flow leading to the steady-state configuration of Bancroft *et al.* They argued that the shock upon entering the material produces an unstable state along the extension of the first-phase Hugoniot. After significant transformation has occurred, the steady-state configuration is approached and the first shock decays to approach the equilibrium transition pressure. Figures 2(a) and 2(b) illustrate this process in the $P-V$ and $P-t$ planes. Recently Novikov *et al.*[7] have suggested a similar explanation of transient flow.

Strength-of-Material Effects

The inherent strength of solid materials leads to a separation of the hydrostatic compression curve and the uniaxial strain curve for compressions up to yielding. If this material strength exists in the plastic region a pressure in excess of the effective hydrostatic pressure would be observed in a material undergoing a phase transformation.

An estimate of this difference of effective pressure can be determined by using an elastic–plastic model and known elastic-constant data. Hydrostatic pressure and the longitudinal stress components are related by

$$\bar{P}=\tfrac{1}{3}(P_x+P_y+P_z). \quad (4)$$

For an isotropic medium where compression is uniaxial along the x axis and where no lateral strain is allowed,[5] Eq. (4) can be written as

$$\bar{P}=P_x-\tfrac{4}{3}(C_s^2/C_l^2)P_{HY} \quad (5)$$

for pressure at or above the yield stress. Here $\bar{P}$ is the hydrostatic pressure, P_x is the longitudinal stress component, and P_{HY} is the Hugoniot elastic limit. In Eq. (5), C_s is the shear sound speed and C_l is the longitudinal sound speed, both measured at ambient temperature and pressure.

Temperature Effects

To completely characterize shock data, an approximation of the temperature attained along the

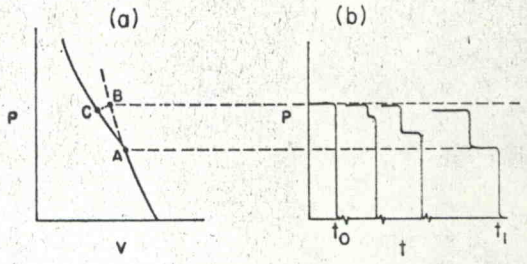

FIG. 2. (a) The Hugoniot of a material which undergoes a phase transformation. Dashed line AB is an unstable extension of the first-phase Hugoniot. Dashed line BC represents a possible line of approach to the steady-state configuration. (b) Wave profiles prior to the establishment of a steady-state flow. The kinetics of the transformation will undoubtedly produce structure behind the first wave for any real material, but the structure is uncertain and is therefore not shown. Here it is assumed that the transformation starts at time t_0 and steady state occurs at a later time t_1. Attenuation of the first wave occurs only between times t_0 and t_1. Attenuation waves propagate forward from the site of transformation until steady flow is obtained.

[7] S. A. Novikov, I. I. Divnou, and A. G. Ivanov, Zh. Eksperim. i Teor. Fiz. **47**, 814 (1964) [English transl.: Soviet Phys.—JETP **20**, 545 (1965)].

Hugoniot by shock heating must be made. At low pressures the shock heating is small, but in the case of a phase transformation where dP/dT is relatively large, temperature calculations are necessary for a proper comparison with the isothermal transition pressure data determined under static loading conditions.

At low pressures, where the Hugoniot and the isentrope are essentially the same, a good estimate of shock heating is obtained with the expression for isentropic compression,

$$T = T_0 \exp[-b(V - V_0)]. \quad (6)$$

To derive this expression $b = (\partial P/\partial T)_v C_v^{-1}$ is assumed constant.[8]

EXPERIMENTAL TECHNIQUES

To determine the thermodynamic parameters which characterize a material at a shock-induced transformation requires a measurement of two of the hydrodynamic quantities U_s, U_p, P, E, or V, and also an assumption about b [Eq. (6)]. The experimental techniques now in use are designed to measure either U_s and U_p or U_s and P. The particle velocity is not generally measured directly, but is approximated at low pressures by assuming that a measured free-surface velocity associated with the wave is twice the particle velocity of the wave. Duff and Minshall in their work on bismuth used simple wire pins placed at various heights from the free surface to determine the free-surface velocity of the various waves. This free-surface data along with the time of shock wave entry into the sample allowed a determination of both U_s and U_p for the shock waves of interest. A quartz-gauge technique recently developed by Graham *et al.*[9] was used in this study.

The piezoelectric current produced in x-cut quartz[10] as a shock wave travels through the quartz is given by

$$i = A(dD/dt) = (kAU_{SQ}/l)[P_0 - P_l] \quad (7)$$

where A is the area of the electrode, dD/t is the displacement current, U_{SQ} is the wave velocity in quartz, l is the thickness of the gauge, P_0 and P_l are the pressures at the front and rear electrodes of the gauge, and k is a coefficient that is independent of time and stress for a given pressure range (see Fig. 3). The quartz-gauge technique allows direct measurement of the pressure in quartz at a quartz-sample interface. Current from x-cut quartz gives in effect a pressure–time profile at the interface during one transit time through the quartz. The gauge response is linear within 2% up to 20 kbar, but gauge uncertainty increases to approximately ±5% at the yield point of x-cut quartz near 50 kbar.

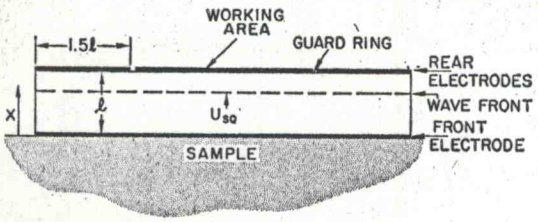

FIG. 3. An x-cut quartz gauge showing the guard-ring configuration. The guard ring maintains one-dimensionality during measurements.

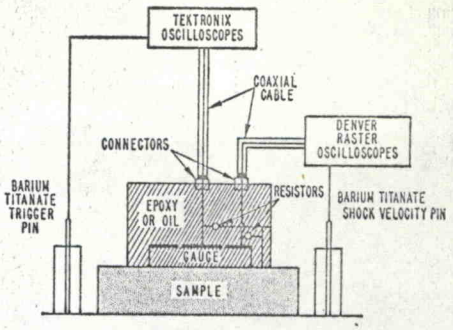

FIG. 4. A typical quartz-gauge experimental configuration.

The electric current produced by the gauge was passed through a resistor (typically 50 Ω) and the voltage was measured on Tektronix 545 or 585 oscilloscopes. The outer electrode signal was passed through a resistor chosen to maintain the same voltage on the outside electrode as occurs on the center electrode. The signal from the outer electrode was used in determining a shock velocity for the sample. Figure 4 illustrates the experimental configuration.

Two sources of shock-induced pressure were available for this study. One was an explosive plane-wave lens system which allowed simultaneous study of as many as five samples. The relatively high detonation pressures generated by the explosives required that attenuation plates be placed between the explosives and the sample to obtain the proper loading pressure. The reproducibility of pressure from a lens system is of the order of 10%, but the wave profiles produced are flat within a few hundredths of a microsecond. The second source of shock pressure was a propellant-driven gun with flat-ended projectiles. This has the disadvantage of limited space for samples, but provides accurate control and measure of input pressure and allows an accurate measure of the shock wave tilt characterizing an experiment.

For these experiments, large discs of cast bsimuth were obtained from United Mineral and Chemical Company. This material was of 99.99% purity and near theoretical density at 9.80 g/cc, but had grains as large as several millimeters across. In one series of experiments the samples that were used were cut directly from the cast stock. To determine any possible effect of

[8] J. M. Walsh and R. H. Christian, Phys. Rev. **97**, 1544 (1955).
[9] R. A. Graham, F. W. Neilson, and W. B. Benedick, J. Appl. Phys. **36**, 1775 (1965).
[10] The quartz gauges that were used to measure the pressures of the various waves were obtained from Valpey Corporation and were ordered to meet the specifications of those used by Graham.

TABLE I. Shock-wave data for bismuth with a quartz pressure gauge. Transitions were at temperatures between 32° and 50°C.

Sample thickness l (mm)	Number of samples	Initial specific volume V_0 (cc/g)	Hugoniot elastic limit P_{HY} (kbar)	Transition-wave shock velocity U_s (mm/μsec)	Transition-wave particle velocity U_p (mm/μsec)	Transition-wave stress P_x (kbar)	Specific volume at the transition V/V_0
Cast bismuth							
1.57–1.78	4	0.1020	2.0±0.6[a]	2.06±0.03	0.126±0.006	25.5±1.1	0.939±0.003
2.49–3.01	7	0.1020	2.1±0.8	2.06±0.03	0.130±0.005	26.5±1.0	0.937±0.003
6.30–6.39	5	0.1020	1.7±0.3	2.06±0.03	0.126±0.006	25.6±1.2	0.939±0.003
9.6–12.7	5	0.1020	2.2±0.3	2.06±0.03	0.12±0.005	24.6±1.0	0.941±0.003
Pressed bismuth							
1.44	1	0.1025	2.5	2.06	0.120	24.5	0.942
2.50–3.26	5	0.1025	2.4±0.2	2.06±0.03	0.124±0.002	25.1±0.4	0.941±0.001
4.52	1	0.1025	2.1	2.06	0.131	26.5	0.937
6.52[b]	2	0.1025	2.4	2.93	0.059	11.5	0.970
Single-crystal bismuth							
a axis							
3.13–4.44	3	0.1020	2.6±0.3	2.06±0.03	0.119±0.001	24.6±0.3	0.942±0.001
c axis							
1.18–4.44	4	0.1020	...	2.06±0.03	0.127±0.003	25.6±0.5	0.939±0.001
1.52[b]	1	0.1020	3.1	1.83	0.067	12.2	0.964

[a] The ± gives the average deviation.

[b] These samples were shock loaded at a pressure below the transition.

grain size on experimental results, a series of experiments were run with samples made by grinding the cast material to a fine powder and then pressing the powder into cylinders of suitable dimensions. The density of these pressed samples was 9.76 g/cc. Single-crystal samples of bismuth were produced by growing long single crystals from the melt. Samples of the desired crystallographic orientation were cut from the large single crystals and were gently lapped to produce flat and parallel surfaces.

RESULTS

The quartz pressure-gauge record for each sample was converted from the original record to a voltage-versus-time plot by the use of vertical and horizontal oscilloscope calibration records. The voltage–time plot was then analyzed according to Eq. (7). The resulting pressure profile in quartz was then converted to a pressure profile in the sample by an impedance-matching technique in which the Hugoniots are assumed linear in the P–U_p plane. This procedure is justified since in the pressure range up to 25 kbar, both the quartz and the bismuth Hugoniots are linear to within 0.5%.

The small ramplike wave which precedes the transition wave through the sample was interpreted as an elastic wave produced by dynamic yielding in the material [see Figs. 5(a) and 5(b). The pressure profile for the elastic wave was determined from more sensitive oscilloscope traces which exhibited the ramplike structure at all thicknesses of the polycrystalline material. This structure cannot be attributed to shock tilt and must therefore arise from increased material strength, which could possibly arise through a dislocation-locking mechanism. The single-crystal samples did not exhibit the ramplike structure but rather a 2.5- to 3-kbar uniform elastic wave. This behavior indicates that the polycrystalline material can yield initially at lower pressures but as plastic flow proceeds the dislocation motion is altered, giving rise to increased material strength. The important step in the elastic-wave analysis was to choose the proper Hugoniot elastic limit from the elastic "wave" produced in the polycrystalline bismuth. The analysis was performed according to an approach suggested by Graham[11] in which the "wave" is analyzed by dividing the sloping line into a number of square waves. The Hugoniot elastic limit determined by this procedure was insensitive to material thickness within experimental error and was in fair agreement with the uniform waves observed on single-crystal samples (see Table I).

Table I gives a compilation of the hydrodynamic data characterizing bismuth in the various experiments.

The uniaxial stress data was converted to an effective hydrostatic pressure by a strength-of-materials correction. The analysis performed on the elastic wave gave a Hugoniot elastic limit in pressed bismuth at a pressure of 2.4±0.2 kbar. When this value for P_{HY}

[11] R. A. Graham (private communication).

was substituted into Eq. (5), along with measured sound speeds, a nonhydrostatic component of 0.8 kbar was obtained.

The single-crystal data were not corrected for strength-of-material effects because of the nonisotropic nature of the bismuth crystal. The single-crystal data are presented as transition stresses. The close agreement of transition stresses between the two orientations indicates that material strength has little effect on the transition.

The c-axis Hugoniot elastic limit was determined in a special experiment, since sound speed along the c axis is less than the 2.06-mm/μsec velocity of the transition wave. The experimentally determined elastic-wave velocity, 1.97 mm/μsec, agrees with the longitudinal sound speed measured before shock loading. The amplitude of the elastic wave was 3.1 kbar.

A calculation of the temperature in bismuth at the point of transition was made for each sample with Eq. (6). A value for b of 11.2 g/cc was used in all of these calculations. To aid in comparison with static data all effective transition pressures were corrected to 25°C by the use of the calculated temperatures and the measured slope of the phase line. A phase line slope of -51 bar/°C was used.

Table II gives a comparison of dynamic data and the accepted static data for the bismuth transition. The values for cast bismuth are listed, but the strength-of-materials correction was made with the ultrasonic data obtained from the pressed samples. This was done because sound speeds in the cast material were not well defined, due to large grain size.

CONCLUSIONS

The results of this detailed study of the Bi I to Bi II phase transformation indicate that the transformation occurs at essentially the same pressure and specific volume under dynamic loading as has been observed under static loading. This agreement obtained after correction of the dynamic data to effective hydrostatic loading indicates that in the case of bismuth the two methods of compression are equivalent. The results further indicate that the bismuth-II transformation under shock loading does not lead to an overpressure resulting from an increased activation-energy barrier.

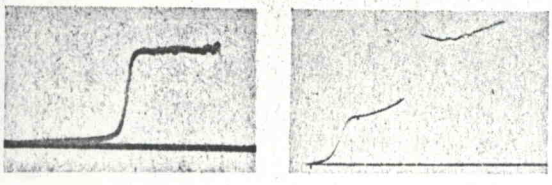

(a) (b)

FIG. 5. (a) A quartz-gauge stress record obtained from shock loading a 6.5-mm-thick sample of cast bismuth. Time increases from left to right. The horizontal line represents zero pressure at the interface. The ramplike wave out in front is the elastic wave which in turn is followed by the transition wave. The driving pressure wave did not arrive at the interface until after transit time through this gauge. (b) This record was obtained from a 1.5-mm-thick pressed sample of bismuth and shows all three waves. The transition wave shows a short plateau region because of the small wave separation in this thin sample.

TABLE II. Bismuth transitions at 25°C with a strength-of-materials correction made on the shock data. The accepted static data are given for comparison.

Experiment	Transition pressure at 25°C $\bar{P}$ (25°C) (kbar)	Specific volume at the transition V/V_0	Hugoniot elastic limit P_{HY} (kbar)
Dynamic			
Cast polycrystals	25.9±1.2	0.939±0.003	2.0±0.6
Pressed polycrystals	25.4±0.8	0.940±0.002	2.4±0.2
Static	25.4±0.1	0.940±0.001	...

The disagreement between this dynamic data and that reported by Duff and Minshall on cast bismuth samples has not been completely explained. Part of the 2.7-kbar difference can be attributed to the 0.8-kbar strength-of-material correction that was made in this study but not in the earlier work. The remaining 1.9-kbar difference is outside of experimental scatter and therefore must be due to a systematic error that characterizes one of the two experimental approaches.

A recent report by Minshall *et al.*[12] points out that a comparison of Minshall's low-pressure pin data with data obtained by other techniques indicates that Minshall's free-surface velocity measurements are in general high. Duff[13] has suggested a possible explanation for these high velocities. He points out that the free-surface pins in Minshall's experiments were separated from the free surface by an air gap. Extreme shock heating caused by reverberation of an air shock across the air gap could possibly serve as a mechanism for electrical breakdown in the gap. If premature shorting of these pins occurred in this way, an apparent higher free-surface velocity could be obtained because of smaller effective gaps. Furthermore, data obtained with the quartz-gauge technique on other materials at low pressures agrees with data obtained by various other free-surface techniques. Therefore, the conclusion is that the previously reported difference between the dynamically and statically observed phase-transition pressures in bismuth is due in part to a strength-of-materials effect and in part to a probable systematic error inherent in the earlier shock-wave experimental technique.

The constancy of the transformation pressure and the sample shock velocity with decrease in sample thickness indicates that steady-state multiple-wave structure is formed very rapidly in the bismuth. Samples as thin

[12] F. S. Minshall, T. R. Loree, and D. Stirpe, "The Overdriving Effects in Dynamic Polymorphism," Los Alamos Scientific Laboratory internal report, 1964 (unpublished).

[13] R. E. Duff (private communication).

as 1.5 mm gave the same results as samples several times as thick. These results indicate that the transformation occurs in times less than or equal to a few nanoseconds.

The experiments on single-crystal bismuth of two different orientations were designed to test the effect of crystal orientation on the transition pressure. The tetragonal structure of Bi I is a small extension of the cube along the c axis. The experimental design was based on the premise that the yet-unknown Bi II structure is cubic and that because of this and the nonhydrostatic compression of the shock experiment, the transformation would occur at a lower pressure along the c axis than along the a axis. The lower average transition pressure observed for a-axis crystals as opposed to c-axis crystals would seem to invalidate the above hypothesis. However, the observed difference for the two crystal-orientations is within experimental scatter. Therefore, the data on single-crystal samples is not conclusive, but it seems to indicate that crystal orientation effects are relatively small.

ACKNOWLEDGMENTS

The author gratefully acknowledges the helpful discussion with Dr. E. Royce and Dr. M. van Thiel and especially Dr. R. E. Duff, who suggested the study. The preparation of single-crystal samples by Dr. H. Conrad and Dr. P. Landon was very much appreciated, as was the work of E. Nidick in fabricating the experimental assemblies.

JOURNAL OF APPLIED PHYSICS VOLUME 38, NUMBER 4 15 MARCH 1967

Diffusion Currents in Large Electric Fields for Discrete Lattices

A. T. FROMHOLD, JR., AND EARL L. COOK*
Department of Physics, Auburn University, Auburn, Alabama
(Received 30 August 1966)

A derivation for the steady-state current J produced by a large homogeneous electric field E_0 in the presence of a concentration gradient is presented which includes explicitly the effects due to lattice discreteness. The resulting equation is

$$J=4a\nu \exp(-W/k_BT)\sinh(ZeE_0a/k_BT)[C(L)-C(0)\exp(ZeE_0L/k_BT)]/[1-\exp(ZeE_0L/k_BT)],$$

where $C(0)$ and $C(L)$ are the boundary concentrations of the diffusing species at the interfaces of the planar film at positions $x=0$ and $x=L$; e, the electronic-charge magnitude; Ze, the charge per particle of the diffusing species; $2a$, the distance between adjacent potential minima; ν, the frequency at which the ion attempts energy barriers which have height W in zero field; k_B, the Boltzmann constant; and T, the absolute temperature. A derivation valid in the limit of a continuum model is also presented, and the results are compared numerically. The equations for the discrete and continuum models reduce to the results predicted by the ordinary linear diffusion equation for electric fields below approximately 10^5 V/cm. The relevance of the equations to the phenomena of anodic and thermal oxidation and to thin-film current–voltage devices is briefly described.

I. INTRODUCTION

THERE are a number of situations for which charged-particle transport is effected by a combination of electric fields and concentration gradients, so current vs voltage is nonohmic. In addition, whenever the electric field is particularly large the current no longer varies linearly with the field, even in the absence of a concentration gradient.

For example, a nonlinear-dependence of ionic current on electric field is experimentally observed in anodic oxidation[1–7] for fields of the order of 10^6 V/cm. This phenomenon was originally observed by Gunterschultze and Betz and explained by Verwey in terms of a significant difference in the potential barriers for forward and reverse ionic motion introduced by the large field.[8] The distance between potential minima deduced from the above hypothesis is not always equal to the lattice constant; this is sometimes interpreted as evidence for a spectrum of jump distances. Alternatively, it has been postulated that the effective charge of the diffusing ion differs from a multiple of the discrete electronic charge because of the partially covalent bonding. The dependence of jump distance on field has been explained by Bean, Fisher, and Vermilyea[2] as a shift in the maximum of the barrier with electric field in the region of the film adjacent to the interface. This is much the same as the corresponding shift in the position of the Schottky barrier maximum for interface-limited electron emission from a metal into a semiconductor or insulator.[9]

---

* NASA Predoctoral Fellow.
[1] L. Young, Proc. Roy. Soc. (London) **A258**, 496 (1960).
[2] C. P. Bean, J. C. Fisher, and D. A. Vermilyea, Phys. Rev. **101**, 551 (1956); D. A. Vermilyea, J. Electrochem. Soc. **102**, 655 (1955).
[3] J. F. Dewald, J. Phys. Chem. Solids **2**, 55 (1957).
[4] N. Sato and M. Cohen, J. Electrochem. Soc. **111**, 512 (1964).
[5] P. H. G. Draper and P. W. M. Jacobs, Trans. Faraday Soc. **59**, 2888 (1963).
[6] R. Dreiner, J. Electrochem. Soc. **111**, 1350 (1964).
[7] L. Young, *Anodic Oxide Films* (Academic Press, Inc., New York, 1961), p. 16.
[8] N. F. Mott, Trans. Faraday Soc. **43**, 429 (1947).
[9] P. R. Emtage and W. Tantraporn, Phys. Rev. Letters **8**, 267 (1962).